

Crystallographic alignment of calcite prisms in the oblique prismatic layer of *Mytilus edulis* shell

Q. L. FENG*, H. B. LI, G. PU, D. M. ZHANG, F. Z. CUI, H. D. LI
 Department of Materials Science and Engineering, Tsinghua University,
 Beijing 100084, People's Republic of China
 E-mail: biomater@mail.tsinghua.edu.cn

T. N. KIM
 Division of Advanced Materials Engineering, Paichai University, Taejon 302-735, Korea

The structure and crystallographic orientation of mineral phase in the oblique prismatic layer of *Mytilus edulis* shell were studied by SEM, XRD and TEM with selected area electron diffraction (SAED). A crystallographic orientation regulation, i.e. the adjacent 1–5 calcite prisms with the same three-dimensional orientation in the oblique prismatic layer, was found for the first time. It is observed that the calcite prisms in the oblique prismatic layer were grown with their (104) parallel to the shell surface.

© 2000 Kluwer Academic Publishers

1. Introduction

Because of their outstanding mechanical properties and complex microstructures, biological hard tissues, such as bone, tooth and mollusk shell, are of considerable materials science interest. Among them, the mollusk shells have been most investigated and the studies on the microstructures and mechanical behaviors have been received great progress [1–5]. It has been found that there are at least seven grossly different types of architecture in mollusk shell, among which the internal lustrous nacreous layer is the best studied [6, 7]. Although the general morphological features of these types are known, the details of the structure of the mineral-organic interface, structure and location of the mineral nuclei are unknown [8, 9]. Recently, the three-dimensional crystal alignment in the nacreous layer was reported [10]. Although it is known that in the prismatic layer of the mollusk, *Atrina serrata* (North Carolina), the long axis of the prisms corresponds to the crystallographic *c*-axis of calcite [11], the crystal orientation relationship between the neighboring prisms in the prismatic layer has not been studied. This information might be invaluable for the accurate understanding of the structure of the prismatic layer and the biomineralization process in mollusk shells. In this paper, we present experimental investigations of the mineral phase structures and crystallographic features of the oblique prismatic layer of the mollusk shell, *Mytilus edulis*, using scanning electron microscope (SEM), X-ray diffraction (XRD) and transmission electron microscope (TEM) with selected area electron diffraction (SAED). A model of crystallographic orientation regu-

lation is proposed to illustrate the growth configuration of the oblique prismatic layer.

2. Experimental

Mature bivalvia mollusc shell, *Mytilus edulis*, grown in the Bohai Sea at Qinhuangdao in North China, was selected for the experiments. They were washed with distilled water and air-dried at room temperature. The cross-sectional fractured specimens were observed under a Hitachi S-450 SEM after deposited with gold films of less than 10 nm.

The plaque (about 1 cm²) of the oblique prismatic layer of the shell was separated mechanically with its surface almost parallel to the surface of the shell under an optical microscope. XRD, using a D/max-RB X-ray diffractometer with 40 keV CuK_α radiation, was employed to analyze the crystal structure and orientation of the oblique prismatic layer.

For investigation by TEM, the ultra-thin segments of the oblique prismatic layer were obtained through mechanical grinding along the direction parallel to the surface of the shell and then by double-side ion milling with a LBS miller. The milling angle was 15° for two hours first and then was 8° about two hours with argon ion (Acceleration voltage 6 kV, milling current 100 μA). During ion milling and TEM investigation the samples were cooled with liquid nitrogen. TEM observation together with SAED was performed using a Hitachi-800 electron microscope operating at 200 kV.

* Author to whom all correspondence should be addressed.

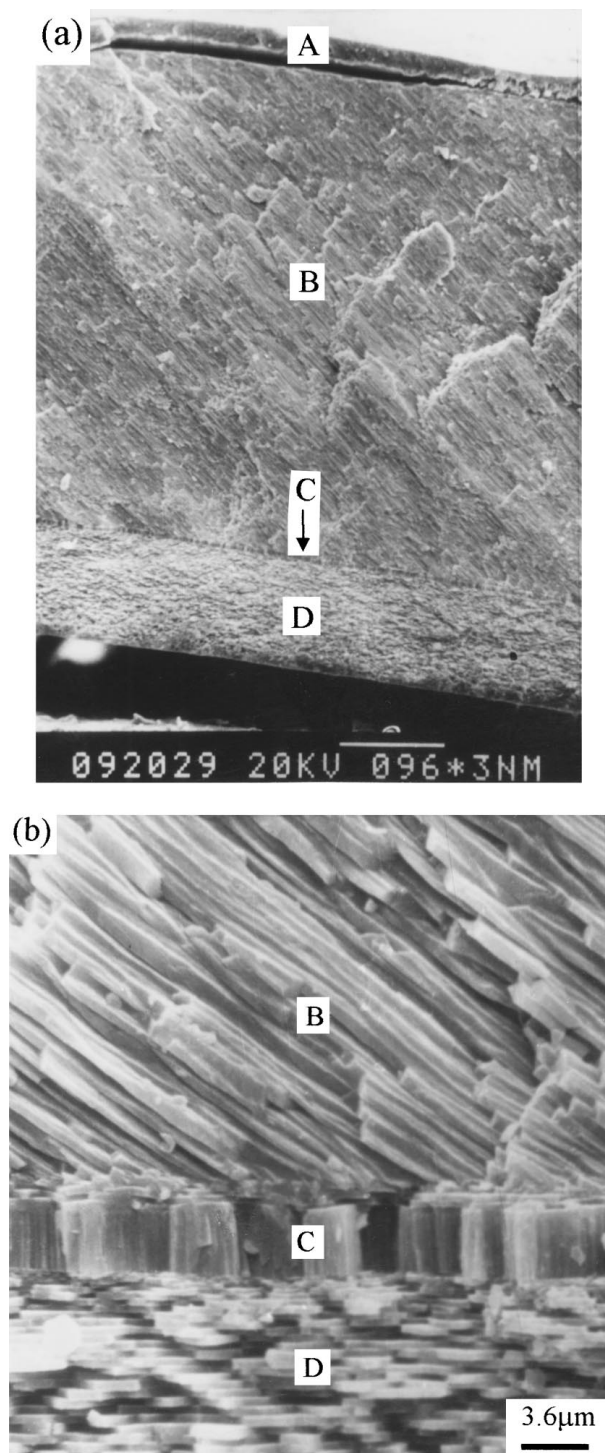


Figure 1 (a) SEM morphology of the cross-section of the shell (A: periostracum, B: oblique prismatic layer discussed in this paper, C: normal prismatic layer, D: nacreous layer); (b) amplified image of (a) showing the structure of the oblique prismatic layer.

3. Results and discussion

Fig. 1 is the SEM image of the cross-section of a *Mytilus edulis* shell showing the structure of its oblique prismatic layer. It can be seen that the fine prisms in the oblique prismatic layer were stacked in the direction of about 45° to the shell surface. The oblique prismatic layer constitutes the major part of the shell (about 80% of the total thickness).

The crystallographic features in the oblique prismatic layer were investigated by TEM with SAED. Fig. 2 is an

example of TEM analysis of specimens in the oblique prismatic layer. Fig. 2a is the TEM micrograph. The tablets in it appear to be narrowly long and oblique to the shell surface. Fig. 2b–d are the SAED patterns of the three neighboring tablets, which are noted in Fig. 2a as B, C and D respectively. The Laue spots in these patterns are corresponding to those of single crystal of calcite. It may be inferred from Fig. 2b–d that the $(10\bar{5})$ of the crystal is perpendicular to the platelet plane since the electron beam is nearly perpendicular to it. Noticed that the angle between the $(10\bar{5})$ and $(10\bar{4})$ is only 6.3° and the angle between the $(10\bar{4})$ and (104) is 90.7° . The appearance of $(10\bar{5})$ rather than $(10\bar{4})$ in these patterns is because that the electron beam used is about 6° to the normal of the platelet plane in order to get explicit diffraction spots. It can be deduced from above that the (104) is parallel to the platelet plane. This deduction is confirmed by the result of XRD. Fig. 3 is the XRD pattern of the specimen of the oblique prismatic layer, which was ground parallel to the shell surface. It can be seen that in this prismatic layer, the crystalline plane with the strongest diffraction intensity of calcite is (104) and the next-to-strongest is (116) , the other peaks are relative weak. Since the specimen was ground parallel to the surface, it is conceivable that the fine prisms in this layer are stacked with (104) parallel to the surface of the shell. Notice that the angle between the (104) and (001) is 44.6° , it is also conceivable that the long axis of the prisms is the crystallographic c -axis of Calcite. Synthetic calcite usually grows as almost isotropic rhombohedra delimited by a set of equivalent oblique $\{104\}$ faces in the hexagonal lattice for that the calcium and carbonate ions are closely packed along these faces to obtain the most thermodynamic stability [12]. Fig. 4 shows the transverse section of fractured oblique prismatic layer. It can be seen that there are many steps in the fractured prisms. These steps have an inclined angle of approximate 45° from the (001) plane. It indicates that the fractured planes are not perpendicular to c -axis in calcite but have a similar orientation as the (104) cleavage plane in calcite. From the fact that the crystals in the oblique prismatic layer were all grown with the (104) parallel to the shell surface, it may indicate that the biomineralization strategy used by the organism is to achieve the minimal growth energy. This preferred orientation of (104) planes can also serve as a mechanical function. Since calcite cleaves easily along the $\{104\}$ planes, the shear stress along the (104) planes parallel to the surface will be the least to avoid the cleavage when the load is exerted in the direction perpendicular to the shell surface.

It is also important to notice that the specimen in Fig. 2 was not rotated in the platelet plane and the diffraction patterns in Fig. 2b–d are uniform. This demonstrates that the crystal orientations of the three neighboring crystals labeled as B, C and D are the same in three-dimension. The two adjacent crystals labeled as E and F in Fig. 2a are also found to have the same orientation, but their diffraction patterns turn around an angle of 3° compared with the patterns in Fig. 2b–d. The same results can also be obtained from other parts of this sample and other samples. Here the adjacent

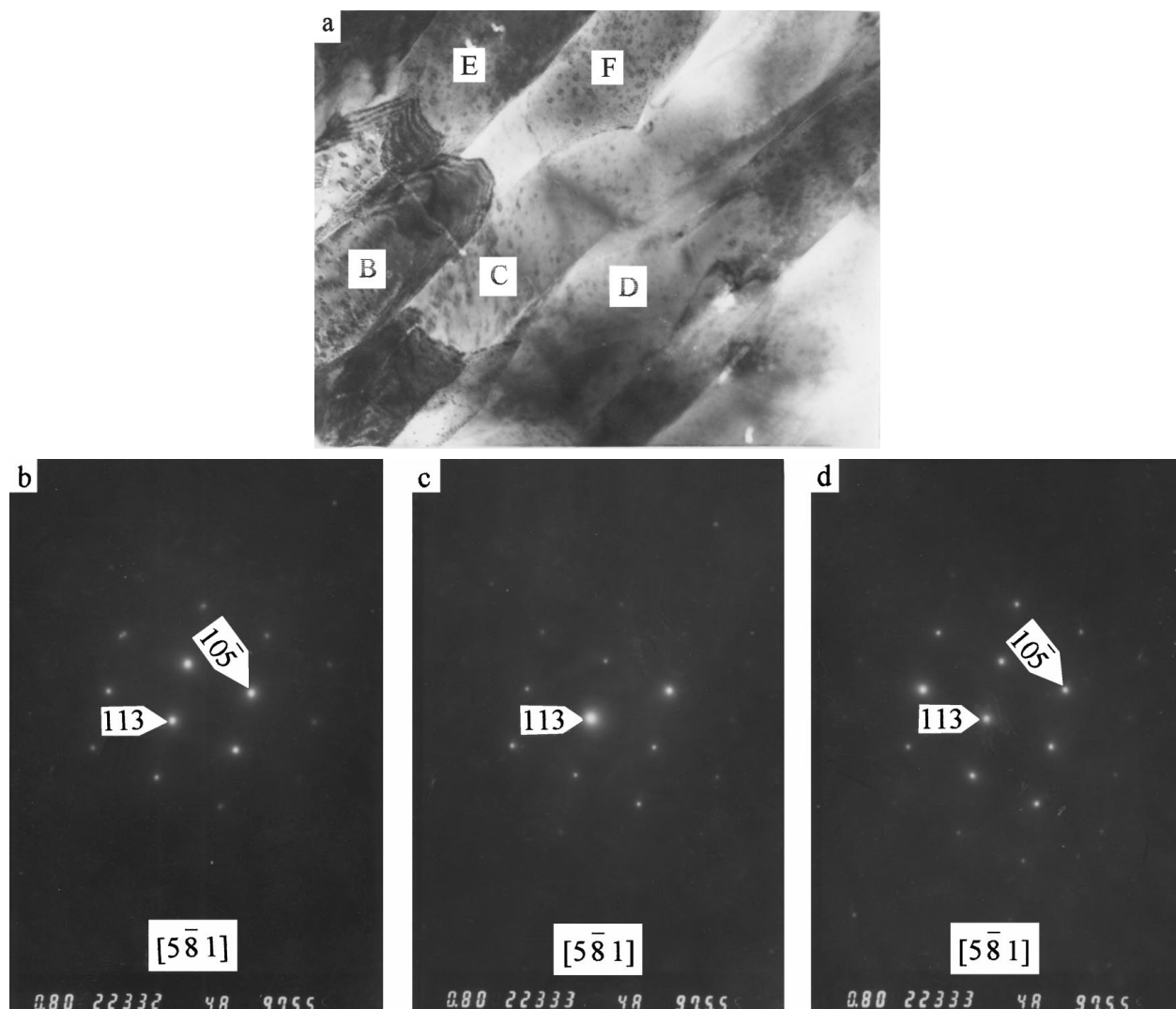


Figure 2 TEM micrograph of the platelet plane of the oblique prismatic layer and corresponding diffraction patterns. (a) TEM micrograph of crystals on platelet plane; (b, c, d) SAED patterns of neighboring crystals labeled B, C and D in (a) respectively. E and F in Fig. 2a are the same oriented crystals whose diffraction patterns are at an angle of 3° to those of B, C and D. Crystalline indices and the corresponding symmetry axis are noted in these patterns.

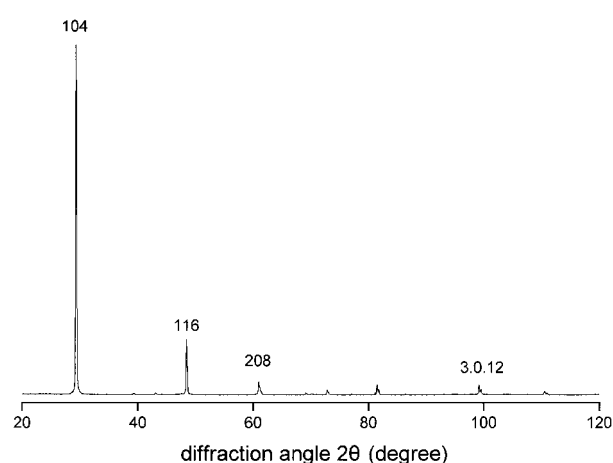


Figure 3 X-ray diffraction patterns of the oblique prismatic layer.

crystals with the same crystal orientation could be named as a domain. The angles between two adjacent differently-oriented domains vary from several degrees to tens of degrees. A crystallographic orientation regulation model is proposed in Fig. 5 to illustrate the

growth configuration of the oblique prismatic layer in the *Mytilus edulis* shell. To the best knowledge of the authors, such a domain structure consisting of 1–5 neighboring crystals with the same three-dimensional orientation in the prismatic layer is found for the first time. Recently Schaffer *et al.* [13] found that the matrix sheets between the successive laminae in the nacreous layer of *Abalone* have pores that both allow the crystals to grow and keep them aligned crystallographically via mineral bridges along the growth direction. The mineral bridges may also exist between the neighboring crystals in the prismatic layer and account for the uniformity of the crystallographic orientation of some adjacent prisms. However, since the prisms were grown simultaneously and are all single crystals, these mineral bridges should exist in the initial part of the prismatic layer.

It is widely believed that the organic matrix serves as the template for the nucleation and growth of biomineralized crystals [14, 15]. The EDTA-insoluble constituents provide an architectural framework covered on both sides by layers of EDTA-soluble constituents, which are aligned with the underlying antiparallel pleated sheet polypeptide chain to provide a structurally

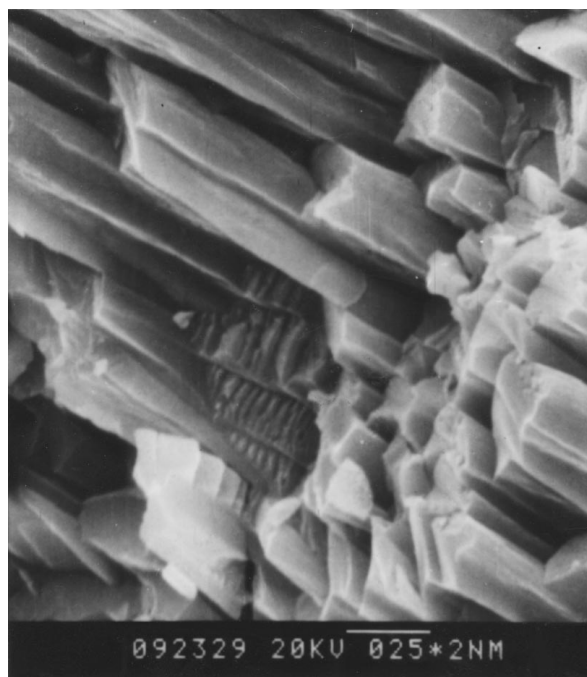


Figure 4 SEM micrograph of the transverse section of fractured oblique prismatic layer.

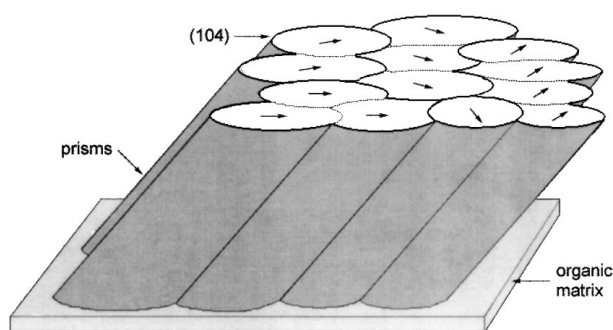


Figure 5 Schematic illustration of the crystallographic orientation regulation of prism growth in the oblique prismatic layer. The direction of the arrows represent some certain crystallographic direction in (104) plane of calcite and the prisms with the same oriented arrows in their (104) planes constitute a domain.

well-defined interface for nucleation [16]. Calcite nucleus can form on the oriented organic template and grow with a defined orientation in space. Weiner and Traub proposed that in the nacreous layer of the gastropod, *Tectus dentatus*, the nucleation site constituted a small part of the total matrix protein sheet structure when compared to the large areas (over $1000 \mu\text{m}^2$) of the appropriate aragonite crystals [17]. It was assumed that the acidic proteins at the nucleation site were also aligned in a regular manner [18]. Some evidences showed that interaction between the crystal surface and the proteins induced oriented crystal nucleation from the {001} plane [19]. We can envisage that in the beginning part of the oblique prismatic layer of *Mytilus edulis*, the nucleating-site regions formed by each mantle epithelium cell would be well aligned over areas ranging from several to tens of square micrometers. Then imagine the following more convincing hypothesis: the organic matrix in the local scale of several micrometers are same aligned to function

as nucleation sites; several calcite nucleation centers with the same orientation develop within this matrix; the subsequent calcite crystals growing on them will be governed along the direction of minimal growth energy, i.e., with the (104) parallel to the surface and in the same three-dimensional orientation to form a domain. Aizenberg et al. implied that protein adsorption and occlusion caused both the observed morphological modifications and anisotropic textural changes [20]. However, little is known about the nucleation site, and hence much of the above discussion is of a speculative nature. More direct investigations should be undertaken to understand the structures of the protein nucleation sites and the crystal growth in the prismatic layer.

Acknowledgement

This work was supported by the National Natural Science Foundation of China, Grant No. 59832070.

References

1. C. GERGOIRE, *The Journal of Biophysical and Biochemical Cytology* **9** (1961) 395.
2. L. J. HUANG and H. D. LI, *Mat. Res. Soc. Symp. Proc.* **174** (1990) 101.
3. V. J. LARAIA, M. AINDOW and A. H. HEUER, *ibid.* **174** (1990) 117.
4. V. J. LARAIA and A. H. HEUER, *J. Am. Ceram. Soc.* **72** (1989) 2177.
5. D. GURUNG and I. KOBAYASHI, *Science Reports of Niigata University* **E 13** (1998) 43.
6. O. B. B ØGGILD, *K. Dan. Vidensk. Selsk. Skr. Naturvidensk. Math. Afd.* **9** (1930) 233.
7. L. ADDADI and S. WEINER, *Nature* **389** (1997) 912.
8. L. ADDADI, J. MORADIAN, E. SHAY, N. G. MAROUDAS and S. WEINER, *Proc. Natl. Acad. Sci. USA* **84** (1987) 2732.
9. M. FRITZ, A. M. BELCHER, M. RADMACHER, D. A. WALTERS, P. K. HANSMA, G. D. STUKY, D. E. MORSE and S. MANN, *Nature* **371** (1994) 49.
10. Q. L. FENG, X. W. SU, F. Z. CUI and H. D. LI, *Biomimetics* **3**(4) (1995) 159.
11. A. BERMAN, J. HANSON, L. LEISEROWITZ, T. F. KOETZLE, S. WEINER and L. ADDADI, *Science* **259** (1993) 776.
12. S. WEINER and L. ADDADI, *J. Mater. Chem.* **7**(5) (1997) 689.
13. T. E. SCHAFFER, C. IONESCU-ZANETTI, R. PROKSCH, M. FRITZ, D. A. WALTERS, N. ALMQVIST, C. M. ZAREMBA, A. M. BELCH, B. L. SMITH, G. D. STUCKY, D. E. MORSE and P. K. HANSMA, *Chem. Mater.* **9** (1997) 1731.
14. G. FALINI, S. ALBECK, S. WEINER and L. ADDADI, *Science* **271** (1996) 67.
15. S. WEINER, Y. TALMON and W. TRAUB, *Int. J. Biol. Macromol.* **5** (1983) 325.
16. S. MANN, *Nature* **332** (1988) 119.
17. S. WEINER and W. TRAUB, *Phil. Trans. R. Soc. Lond.* **B 304** (1984) 425.
18. L. ADDADI and S. WEINER, *Angew. Chem. Int. Engl.* **31** (1992) 153.
19. S. ALBECK, J. AIZENBERG, L. ADDADI and S. WEINER, *J. Am. Chem. Soc.* **115** (1993) 11691.
20. J. AIZENBERG, J. HANSON, T. F. KOETZLE, S. WEINER and L. ADDADI, *ibid.* **119** (1997) 881.

Received 27 April
and accepted 23 November 1999